Supporting Information

MATERIALS AND METHODS

Materials Agarose II (Amresco, Solon, OH). 1,2-dioleoyl-*sn*-glycero-3-phosphocholine (DOPC), 1,2-dipalmitoyl-*sn*-glycero-3-phosphoethanolamine-N-(lissamine rhodamine B sulfonyl) (Rhodamine-PE) (PC, Avanti Polar Lipids, Alabaster, AL). Calcium chloride dihydrate (BDH Chemicals, Westchester, PA). Strontium chloride hexahydrate (Alfa Aesar, Ward Hill, MA). Barium chloride dehydrate (EMD Millipore, Billerica, MA). Ammonium carbonate, Sodium chloride, Dichloromethane (Mallinckrodt Baker, Phillipsburg, NJ). Calcein (TCI America, Portland, OR). Molecular Porous Membrane Tubing (MWCO: 3500, Spectrum Laboratories, Rancho Dominguez, CA). Unless otherwise noted, all solutions where prepared in ultra-pure water (ρ = 18.2 MΩ cm) prepared with a Barnstead NanoDiamond UF + UV purification unit.

Liposome preparation. The procedure for the preparation of giant liposomes was adapted from Horger and coworkers.[1] Agarose films were deposited on a glass coverslip by dip coating one side of the glass onto the surface of a melted 1 wt% agarose solution. The agarose films were then dried at 40°C overnight in a convection oven. The lipid films were deposited by pipetting 50 µL of 5 mg/mL lipids in dichloromethane onto the agarose-coated coverslip. Dichloromethane was removed by placing the films under vacuum for at least 20 min. To form liposomes the lipid+agarose films were rehydrated by submerging the coverslips in 1 mL of aqueous $CaCl_2$, $SrCl_2$ or $BaCl_2$ for 1 h. The concentrations of the $CaCl_2$, $SrCl_2$ or $BaCl_2$ solutions were 1.0, 0.17, and 0.77 M, respectively (see below for a discussion of the supersaturation). To remove unencapsulated cations the resulting liposome suspension was dialyzed against 500 mL of isosmotic aqueous NaCl. The dialysis bath was replaced 4 times over 24 h.

Precipitation inside liposomes. Precipitation of calcium, strontium, and barium carbonate inside the giant liposomes was initiated by gentle mixing of 800 µL of liposome suspension with 200 µL of 1.5 M $(NH_4)_2CO_3$ for a final concentration of 300 mM $(NH_4)_2CO_3$. Liposome suspensions were imaged in a Leica DMI6000B microscope equipped with polarized light optics. Due to the small size and rapid movement of initial precipitates of witherite ($BaCO_3$), their birefringence is difficult to capture, but is obvious when observed by eye.

Supersaturation inside liposomes. Assuming that equilibration outside the liposome, transport CO_2 and NH_3 across the membrane, and equilibration inside the liposome are fast compared to the timescale of phase transformation, and neglecting activity coefficients and pH effects, the maximum possible supersaturation for the crystalline polymorphs calcite, strontianite, and witherite inside the liposomes is $\sigma = \ln([M^{2+}][CO_3^{2-}]/K_{sp}) \sim 18$ for all three cations. Accounting for speciation and activity using Visual MINTEQ, we expect upper limits for the supersaturation $\sigma_{calcite} \leq 10.8$, $\sigma_{strontianite} \leq 12$, and $\sigma_{witherite} \leq 11.5$. Please note that there will be a time interval during which the supersaturation increases rapidly, and that the final value may not be reached if an amorphous carbonate precipitates early in the process. Given that precursor growth is fast compared to trans-membrane transport,[2] the supersaturation inside liposomes after formation of the precursor will remain approximately constant and close to $\sigma = \ln(K_{sp,amorphous}/K_{sp,\ crystalline})$. For ACC and calcite, we calculate $\sigma = 4.8$ based on $pK_{sp\_ACC} = 6.4$[3] or $\sigma = 5.6$ based on $pK_{sp\_ACC} = 6.04$.[4] While the overall development of the supersaturation over time for $SrCl_2$ and $BaCl_2$-loaded liposomes is likely similar, in the absence of solubility data for the amorphous carbonates, equivalent supersaturation values cannot be calculated (see section 3 in the supporting discussion).

Lysis of liposomes. Lysis of phospholipid membrane was performed 4 h from the addition of ammonium carbonate, by addition of 100 µL of 30 wt% Triton-X to 900 µL of liposome suspension.

Raman microscopy. Confocal Raman spectra were recorded using a WITec Confocal Raman spectrophotometer, in backscattering configuration. Spectra from bulk reference standards and liposome-stabilized ACC were measured using a Nikon 20x objective and 60x water immersion objective, respectively. All spectra were collected using a 532 nm fiber optic laser for excitation and a 60 s integration time.

Scanning electron microscopy. 50 µL of liposome suspension was deposited on a silicon wafer and excess solution removed by wicking with filter paper. Residual salt was washed with 50 µL of ultrapure water. Samples were air dried in a vacuum desiccator for 30 min before coating with 10 nm of Au/Pd. The samples were imaged at 5 and 20 kV in a Hitachi S4800 scanning electron microscope.

Confocal Microscopy. Giant liposomes were prepared from 5 mg/mL lipid solutions containing 0.5 wt% rhodamine-PE. For observation of the ACC precipitates the lipids films were rehydrated with aqueous 1 M $CaCl_2$ solutions containing 20 µg/mL calcein. To observe agarose incorporation, the agarose film was fluorescently labeled with fluorescein isothiocyanate following the procedure of Horger et al.[1] Liposomes were

imaged using a Zeiss 510 Meta/ConfoCor3 system. Fluorescence from rhodamine-PE was excited using the 543 nm line of HeNe. Fluorescence from calcein and fluorescein was excited using the 488 nm line of Argon.

SUPPORTING DISCUSSION

1. The role the liposome membrane and agarose in stabilizing ACC.

The inner leaflet of the membrane provides a surface that may play a role in the formation and/or stabilization of ACC. In addition, some agarose present during liposome formation may be encapsulated in the liposomes. We therefore used confocal microscopy to investigate where ACC forms and whether it interacts with the lipid membrane or agarose. Precipitation experiments were performed in liposomes containing 0.5 wt% rhodamine-labeled PE that were a) loaded with both Ca^{2+} and the fluorescent dye calcein (SI Figure 1); or b) prepared on fluorescein-labeled agarose films (SI Figure 2). After addition of a solution of $(NH_4)_2CO_3$ to Ca^{2+} and calcein loaded liposomes, highly fluorescent, calcein-labeled ACC nanoparticles form throughout the lumen, confirming results from bright field microscopy. It is thus clear that ACC does not preferentially form at the membrane. Optical sections through the liposome volume at 4 h (SI Figure 1) show that ACC nanoparticles have loosely aggregated at the bottom of the liposome rather than coating the entire membrane surface. This suggests that that interaction between ACC and the PC membrane is weak.

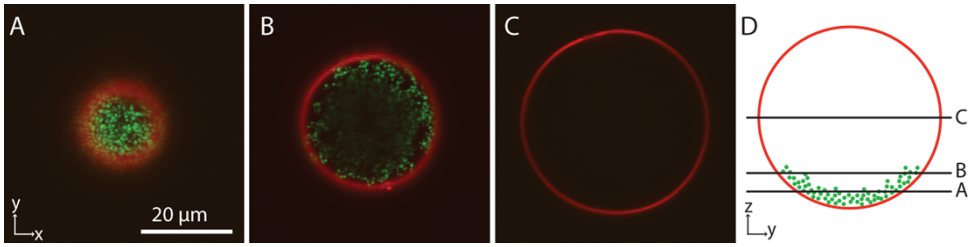

SI Figure 1: (A, B, C) Optical sections of a giant PC liposome (red) with encapsulated ACC nanoparticles (green) at 4h. (D) Approximate location of the sections A-C. Precipitation experiments were performed in liposomes containing 0.5wt% rhodamine-labeled PE and loaded with both Ca^{2+} and calcein.

In liposomes prepared from fluorescein-labeled agarose films, fluorescein is confined to the phospholipid membrane (SI Figure 2), and is absent from the lumen of the liposome. This suggests that while a small amount of agarose is incorporated into the lamellae of multilamellar giant liposomes, it is excluded from the precipitate and does not play role in the nucleation and stabilization of ACC.

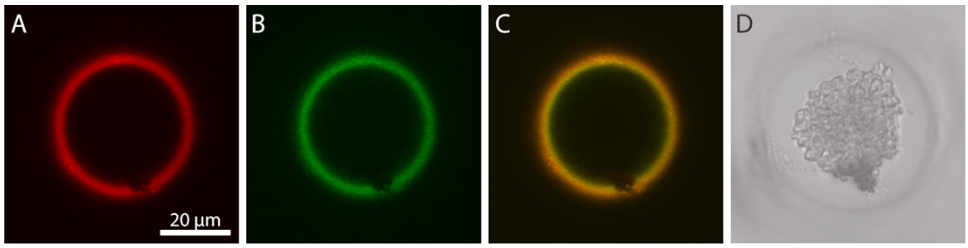

SI Figure 2: Confocal microscopy images of (A) the phospholipid membrane with 0.5% rhodamine-PE (red), (B) agarose labeled with FITC (green), and (C) composite of the two images in which agarose colocalized with membrane appears yellow. The optical sections were recorded from the bottom half of the liposome. The location of the ACC precipitate is visible in the bright field image (D) recorded from the same focal plane.

2. Characterization of precipitates in liposome by Raman microscopy.

In situ confocal Raman spectra of precipitates formed in liposomes loaded with $CaCl_2$ show the typical features of bulk synthetic ACC (Figure 2 in the main text).[5] The ν_1 mode at 1080 cm^{-1} is significantly broadened compared to that of calcite and aragonite, and the characteristic splitting of vaterite is not observed. The ν_4 mode characteristic for calcite (711 cm^{-1}) and vaterite (6 bands between 660-780 cm^{-1}) is absent.[6] Individual lattice mode vibrations characteristic of the crystalline polymorphs are similarly absent and replaced by a very broad peak at 50-300 cm^{-1}.

In situ confocal Raman spectra of birefringent precipitates formed in liposomes loaded with $SrCl_2$ closely match spectra recorded from bulk strontianite powder, those of precipitates in $BaCl_2$-loaded liposomes match spectra of a synthetic witherite reference standard (SI Fig. 3).

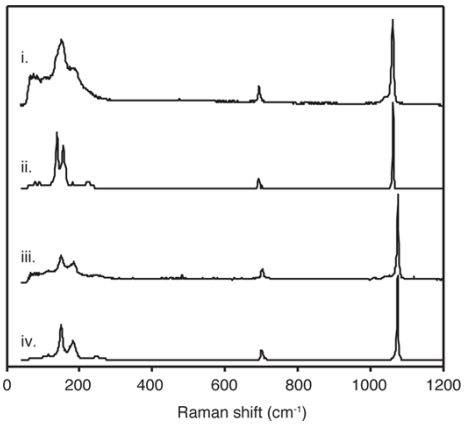

SI Figure 3: Raman spectra recorded in situ of (i) a strontianite precipitate in a giant liposome, (ii) strontiante reference powder, (iii) a witherite precipitate in a giant liposome, and (iv) witherite reference powder.

3.Trends in the solubility and stability of the amorphous alkaline earth carbonates

A necessary condition for precipitation of any of the amorphous carbonates is that this lowers the free energy of the system. For the phase to be observable its lifetime needs to be sufficiently long on the experimental timescale, which in our case is in the range of seconds and longer. Under the assumption that growth of the crystalline polymorphs is much faster than nucleation, this requires that the barrier to formation of the amorphous phase is lower than the reversible work of nucleation (W*) of the crystalline phase. Note that if the formation of the amorphous phase proceeds by spinodal decomposition, the former barrier vanishes.

Based on the data of others and our observations,[7-8] these conditions are fulfilled for both ACC and ASC. While ACC has a long lifetime, at least $7 \cdot 10^5$ s (8 days), the lifetime of ASC is in the hundreds of seconds. There is indirect evidence for the formation of ABC,[7-8] but we did not observe formation, which indicates that its lifetime – if its forms at all under the conditions in our system – is significantly below seconds. It is of course also possible that the free energy for the formation of ABC is much smaller (its solubility higher) than that of ASC and ACC, such that either very little is formed only, or that the free energy change of its formations is positive such that does not form spontaneously. While it is not possible to separate the effect of the differences in the stability (solubility) of the amorphous carbonates from the kinetic effects based on the available data, we note that there is a general trend to shorter lifetimes with increasing ionic radius.

This correlation may result from the position of Ca^{2+} at the threshold size where it can form both rhombohedral (calcite, vaterite) and orthorhombic carbonates (aragonite), as well as hydrous and anhydrous carbonates.[9] Reeder and coworkers have suggested a structural model for ACC in which this ability of Ca^{2+} and CO_3^{2-} form many structurally different but energetically similar coordination geometries is clearly apparent.[10] One can think of this phenomenon as frustrating attempts to form a crystalline lattice and stabilizing the amorphous carbonate (lowering its free energy/solubility). With increasing radius, Sr^{2+} and Ba^{2+} increasingly favor just one coordination environment, that of orthorhombic aragonite. Consequently, we expect the free energy of the amorphous carbonates to become less negative with increasing cation radius and their solubility to increase. Considering that synthetic ACC contains stoichiometric amounts of water, this trend is likely amplified by the weaker binding of water by Sr and Ba.[11]

An increase in the solubility of ASC compared to ACC combined with the lower solubility of strontianite (pK_{sp} = 9.25 at 298 K)[12] compared to calcite (pK_{sp} = 8.48 at 298 K)[12] would then result in a higher supersaturation with respect to the formation of strontianite both before and especially after the formation of ASC. This is consistent with the reduced lifetime of ASC compared to ACC. Given that the solubility of witherite (pK_{sp} = 8.59 at 298 K)[12] is close to that of calcite, ABC would have to be quite a few orders of

magnitude more soluble than ACC for the supersaturation with respect to witherite to become large enough to reduce the barrier to nucleation sufficiently for the fast rate of formation that we observe.

REFERENCES

[1] Horger, K. S., Estes, D. J., Capone, R., Mayer, M., *J. Am. Chem. Soc.* **2009**, *131*, 1810-1819. "*Films of Agarose Enable Rapid Formation of Giant Liposomes in Solutions of Physiologic Ionic Strength.*"

[2] Tester, C. C., Wu, C.-H., Weigand, S., Joester, D., *Faraday Disc* **2012**, *159*, 345-356. "*Precipitation of ACC in liposomes-a model for biomineralization in confined volumes.*"

[3] Brecevic, L., Nielsen, A. E., *J. Cryst. Growth* **1989**, *98*, 504-510. "*Solubility of amorphous calcium-carbonate.*"

[4] Clarkson, J. R., Price, T. J., Adams, C. J., *Journal of the Chemical Society-Faraday Transactions* **1992**, *88*, 243-249. "*Role of metastable phases in the spontaneous precipitation of calcium-carbonate.*"

[5] Addadi, L., Raz, S., Weiner, S., *Adv. Mater.* **2003**, *15*, 959-970. "*Taking advantage of disorder: Amorphous calcium carbonate and its roles in biomineralization.*"

[6] Wehrmeister, U., Soldati, A. L., Jacob, D. E., Haeger, T., Hofmeister, W., *JRSp* **2010**, *41*, 193-201. "*Raman spectroscopy of synthetic, geological and biological vaterite: a Raman spectroscopic study.*"

[7] Homeijer, S. J., Barrett, R. A., Gower, L. B., *Crystal Growth & Design* **2010**, *10*, 1040-1052. "*Polymer-Induced Liquid-Precursor (PILP) Process in the Non-Calcium Based Systems of Barium and Strontium Carbonate.*"

[8] Wolf, S. E., Müller, L., Barrea, R., Kampf, C. J., Leiterer, J., Panne, U., Hoffmann, T., Emmerling, F., Tremel, W., *Nanoscale* **2011**, *3*, 1158-1165. "*Carbonate-coordinated metal complexes precede the formation of liquid amorphous mineral emulsions of divalent metal carbonates.*"

[9] Railsback, L. B., *Carbonates and Evaporites* **1999**, *14*, 1-20. "*Patterns in the compositions, properties, and geochemistry of carbonate minerals.*"

[10] Goodwin, A. L., Michel, F. M., Phillips, B. L., Keen, D. A., Dove, M. T., Reeder, R. J., *Chem. Mater.* **2010**, *22*, 3197-3205. "*Nanoporous Structure and Medium-Range Order in Synthetic Amorphous Calcium Carbonate.*"

[11] Binder, H., Zschornig, O., *Chem. Phys. Lipids* **2002**, *115*, 39-61. "*The effect of metal cations on the phase behavior and hydration characteristics of phospholipid membranes.*"

[12] *CRC Handbook of Chemistry and Physics*, 93rd ed. (Ed.: Haynes, W. M.), CRC Press/Taylor and Francis, Boca Raton, FL, **2013**.